



Metal–Inorganic Frameworks Hot Paper

How to cite: *Angew. Chem. Int. Ed.* **2020**, *59*, 10321–10326

International Edition: doi.org/10.1002/anie.202002487

German Edition: doi.org/10.1002/ange.202002487

High-Pressure Synthesis of Metal–Inorganic Frameworks $\text{Hf}_4\text{N}_{20}\cdot\text{N}_2$, $\text{WN}_8\cdot\text{N}_2$, and $\text{Os}_5\text{N}_{28}\cdot 3\text{N}_2$ with Polymeric Nitrogen Linkers

Maxim Bykov,* Stella Chariton, Elena Bykova, Saiana Khandarkhaeva, Timofey Fedotenko, Alena V. Ponomareva, Johan Tidholm, Ferenc Tasnádi, Igor A. Abrikosov, Pavel Sedmak, Vitali Prakapenka, Michael Hanfland, Hanns-Peter Liermann, Mohammad Mahmood, Alexander F. Goncharov, Natalia Dubrovinskaia, and Leonid Dubrovinsky

Abstract: Polynitrides are intrinsically thermodynamically unstable at ambient conditions and require peculiar synthetic approaches. Now, a one-step synthesis of metal–inorganic frameworks $\text{Hf}_4\text{N}_{20}\cdot\text{N}_2$, $\text{WN}_8\cdot\text{N}_2$, and $\text{Os}_5\text{N}_{28}\cdot 3\text{N}_2$ via direct reactions between elements in a diamond anvil cell at pressures exceeding 100 GPa is reported. The porous frameworks (Hf_4N_{20} , WN_8 , and Os_5N_{28}) are built from transition-metal atoms linked either by polymeric polydiazenediyl (polyacetylene-like) nitrogen chains or through dinitrogen units. Triply bound dinitrogen molecules occupy channels of these frameworks. Owing to conjugated polydiazenediyl chains, these compounds exhibit metallic properties. The high-pressure reaction between Hf and N_2 also leads to a non-centrosymmetric polynitride Hf_2N_{11} that features double-helix catenapoly[tetraz-1-ene-1,4-diyl] nitrogen chains $[-\text{N}=\text{N}-\text{N}=\text{N}-]_\infty$.

Homoatomic bonding, being a prominent feature of carbon chemistry, is also characteristic for pnictogens, which readily form extended polymers and homoatomic frameworks.^[1,2] Contrary to carbon and phosphorus, the nitrogen–nitrogen single and double bonds possess much less than 1/3 and 2/3, respectively, of the energy of the triple bond. Therefore, the conversion of N–N single or double bonds to triple bonds results in a very large energy release and makes the polynitrides highly endothermic and thermodynamically

unstable at atmospheric pressure. At high pressures, however, the decomposition of such phases with the evolution of nitrogen is efficiently suppressed that provides a playground for systematic studies of nitrogen-rich compounds, in which various nitrogen-containing polyanions can be stabilized by simple metal cations. Even if such compounds may appear to be unstable at ambient conditions, high-pressure experiments provide a proof of their existence and valuable information for further development of the ambient-pressure synthesis of nitrogen-rich phases. So, the first successful synthesis of alkali metal pentazoles (salts containing *cyclo*- N_5^- anions) was performed at high pressure.^[3] Later, unsubstituted *cyclo*- N_5^- was stabilized at ambient conditions too.^[4–8] Metal–pentazolate frameworks (AgN_5 , $\text{Cu}(\text{N}_5)(\text{N}_3)$,^[6,9] $\text{Na}_{24}\text{N}_{60}$, $\text{Na}_{20}\text{N}_{60}$ ^[5]) might not only have applications as energetic materials, but also be intrinsically interesting as direct inorganic structural analogues of azolate metal–organic frameworks and framework materials based on an aromatic inorganic linker.^[9,10] Metal–azide frameworks based on transition metals linked through bridging azido ligands are important for the development of molecular magnets.^[11,12]

Recent high-pressure studies have shown that various polynitrogen species may occur as a result of simple reaction between a metal and molecular nitrogen. Good examples of that are FeN_4 containing catena-poly[tetraz-1-ene-1,4-diyl]

[*] Dr. M. Bykov, Prof. M. Mahmood
Department of Mathematics, Howard University
2400 Sixth Street NW, Washington, DC 20059 (USA)
E-mail: maks.byk@gmail.com

Dr. M. Bykov, S. Khandarkhaeva, Prof. L. Dubrovinsky
Bayerisches Geoinstitut, University of Bayreuth
Universitätsstrasse 30, 95440 Bayreuth (Germany)

Dr. M. Bykov, Dr. E. Bykova, Dr. A. F. Goncharov
The Earth and Planets Laboratory, Carnegie Institution for Science
5241 Broad Branch Road, NW, Washington, DC 20015 (USA)

Dr. S. Chariton, Dr. V. Prakapenka
Center for Advanced Radiation Sources, University of Chicago
9700 South Cass Avenue, Lemont, IL 60437 (USA)

T. Fedotenko, N. Dubrovinskaia
Material Physics and Technology at Extreme Conditions
Laboratory of Crystallography, University of Bayreuth
Universitätsstrasse 30, 95440 Bayreuth (Germany)

A. V. Ponomareva
Materials Modeling and Development Laboratory
National University of Science and Technology “MISIS”
119049 Moscow (Russia)

J. Tidholm, F. Tasnádi, I. A. Abrikosov, N. Dubrovinskaia
Department of Physics, Chemistry and Biology (IFM)
Linköping University, 58183 Linköping (Sweden)

P. Sedmak, M. Hanfland
European Synchrotron Radiation Facility
BP 220, 38043 Grenoble Cedex (France)

H.-P. Liermann
Photon Science, Deutsches Elektronen-Synchrotron
Notkestrasse 85, 22607 Hamburg (Germany)

Supporting information and the ORCID identification number(s) for the author(s) of this article can be found under:
<https://doi.org/10.1002/anie.202002487>

© 2020 The Authors. Published by Wiley-VCH Verlag GmbH & Co. KGaA. This is an open access article under the terms of the Creative Commons Attribution License, which permits use, distribution and reproduction in any medium, provided the original work is properly cited.

anions $[-N=N-N-N-]_{\infty}^{2-}$,^[13,14] MgN_4 , and $ReN_8 \cdot N_2$ with polydiazenediyl (polyacetylene-like) nitrogen chains.^[15,16] Thus, high-pressure synthesis conditions enable the exploration of numerous possible metal–nitrogen framework topologies.

Herein we studied chemical reactions between 5d transition metals Hf, W, Os, and nitrogen in laser-heated diamond anvil cells at pressures exceeding 1 Mbar. All metals were found to form metal–inorganic frameworks MIFs: $Hf_4N_{20} \cdot N_2$ (**1**), $WN_8 \cdot N_2$ (**2**), $Os_5N_{28} \cdot 3N_2$ (**3**) with polymeric nitrogen linkers and guest dinitrogen molecules that are arranged in one-dimensional arrays. In all experiments discussed herein, a piece of metal was placed inside a sample chamber in a BX90 diamond anvil cell^[17] loaded with nitrogen that served as a reagent and as a pressure-transmitting medium. Hf, W, and Os samples were compressed to a pressure of about 105 GPa and laser-heated to 1900(200), 2700(200), and 2800(150) K, respectively. The reaction products contained multiple good-quality single-crystalline domains of novel phases, which were studied using synchrotron single-crystal X-ray diffraction (SCXRD) at the beamlines P02.2 (PetraIII, DESY, Hf sample), GSECARS 13IDD (APS, W and Hf samples), ID15b (ESRF, W sample) and ID11 (ESRF, Os sample). More details on the experimental procedures are given in the Supporting Information.

The crystal-structure solution and refinement revealed the chemical formulas of new compounds as $Hf_4N_{20} \cdot N_2$, $WN_8 \cdot N_2$ and $Os_5N_{28} \cdot 3N_2$ (Figure 1). The refinement against SCXRD data resulted in very good agreement factors (Supporting Information, Table S1). For a cross-validation of the crystal structures we performed theoretical calculations based on density functional theory. We carried out the full structure optimization for all of the compounds from ambient to the synthesis pressure and found that optimized crystal structures are in a very good agreement with the experimental ones (Supporting Information, Table S2).

The structure of $WN_8 \cdot N_2$ has the orthorhombic space group *Immm* with one W and two N atomic positions. $WN_8 \cdot N_2$ is isostructural to previously reported inclusion compound $ReN_8 \cdot N_2$.^[15] W atoms are eightfold coordinated by four planar polydiazenediyl nitrogen chains with conjugated π -systems (Figure 1g, Scheme 1). The 3D framework WN_8 possesses rectangular-shaped channels that are occupied by dinitrogen

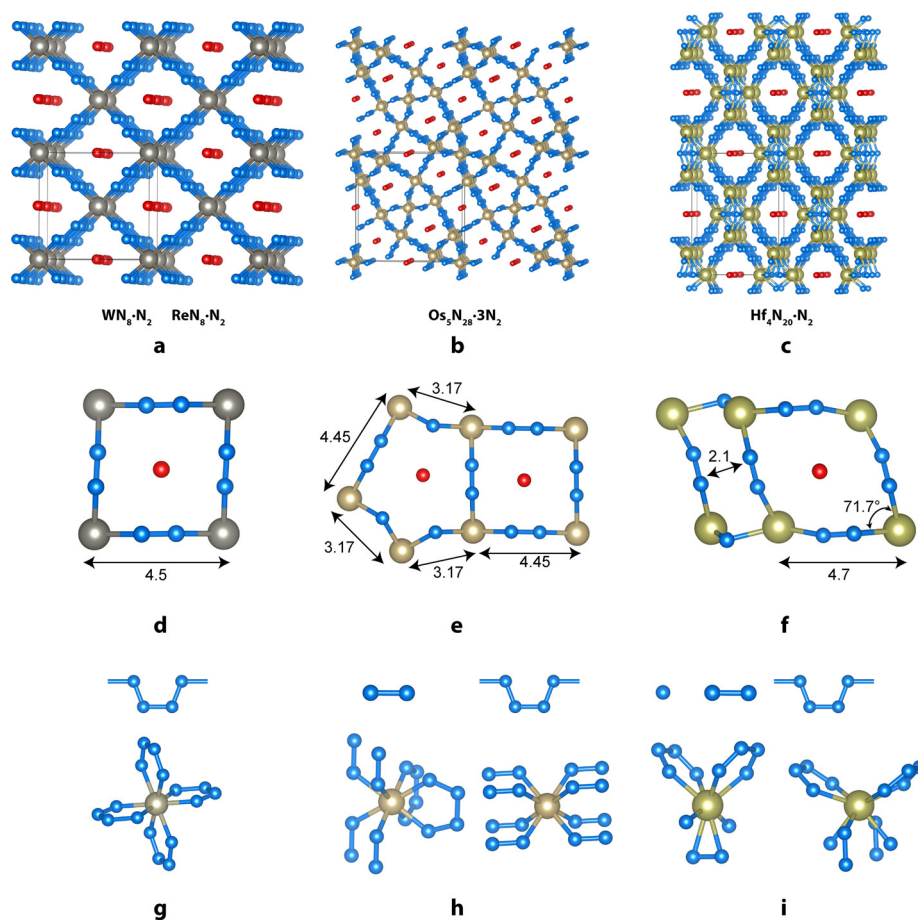
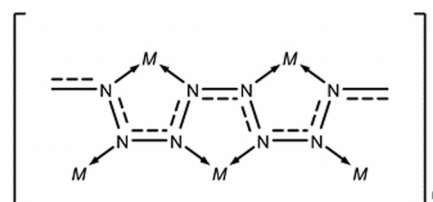


Figure 1. a)–f) Crystal structures of a) $WN_8 \cdot N_2$, b) $Os_5N_{28} \cdot 3N_2$, and c) $Hf_4N_{20} \cdot N_2$, and geometries of the channels in the crystal structures (d–f). Distances are given in Å. g)–i) Types of nitrogen units building the network and types of metal coordination in corresponding compounds. Blue spheres represent nitrogen atoms that are the part of the framework. Red spheres represent dinitrogen molecules confined in the channels. Larger spheres represent corresponding transition metals.



Scheme 1. Coordination of metal atoms by a polydiazenediyl (polyacetylene-like) nitrogen chain.

molecules (Figure 1d). In the ionic consideration, each W atom gives four of its six valence electrons to four N_4 units. Thus, each N_4 unit accommodates 2 electrons and has 22 valence electrons in total: four N–N σ bond pairs (8e), four dative N→W bonds (8e), and six π -delocalized electrons with an effective N–N bond order of 1.25. Tungsten, therefore, should have a formal oxidation state +IV and the formula of the framework can be written as $W^{4+}(N_4^{2-})_2$. The framework topology can be described by a point symbol $\{5^2.6\}_8\{5^4.6^{12}.9^{12}\}$ as determined by the software ToposPro.^[18]

The structure of $\text{Os}_5\text{N}_{28}\cdot 3\text{N}_2$ has the orthorhombic space group $Pnmm$ with 3Os and 9N atomic positions. It exhibits two types of nitrogen units: N–N dumbbells and polydiazenediyl chains, so that the chemical formula of the framework may be rewritten as $\text{Os}_5(\text{N}_2)_6(\text{N}_4)_4$. The nitrogen–nitrogen distances within the dumbbells vary in a range 1.22–1.33 Å, which is characteristic for a double bond of the $[\text{N}=\text{N}]^{2-}$ unit. This is in a good agreement with the common oxidation state of osmium +IV and the formula of the framework can be written as $(\text{Os}^{4+})_5(\text{N}_2^{2-})_6(\text{N}_4^{2-})_4$. All Os atoms possess distorted cubic coordination by nitrogen atoms. Os1 atoms are coordinated only by nitrogen atoms that form dumbbells, while Os2 and Os3 atoms are coordinated by both type of units in the proportion 1:1 (Figure 1h). The framework contains rectangular and octagonal-shaped channels occupied by dinitrogen molecules. The framework topology can be described by a point symbol $\{4.6^2\}_{12}\{4^2.5^2.6^{14}.8^8.9^2\}_4\{4^4.6^{16}.8^8\}_{5^2.6\}_{16}$.

The structure of $\text{Hf}_4\text{N}_{20}\cdot \text{N}_2$ has the orthorhombic space group $Cmmm$ with 2 Hf and 5 N atomic positions. Among all reported compounds, $\text{Hf}_4\text{N}_{20}\cdot \text{N}_2$ has the highest number of various nitrogen units: polydiazenediyl nitrogen chains, N–N dumbbells, and discrete N atoms. Nitrogen–nitrogen distances within the dumbbells are 1.32 Å and, therefore, the formula can be written as $(\text{Hf}^{4+})_4(\text{N}^{3-})_2(\text{N}_2^{2-})(\text{N}_4^{2-})_4$ with Hf^{4+} in good agreement with the most common oxidation state of Hf (+IV). The framework contains rhombus-shaped channels occupied by dinitrogen molecules. The framework topology can be described by the point symbol $\{3.4^4.5^6.6^3.7^8.8^4.9^2\}\{3^2.4^5.5^3\}\{4^5.5^6.6^3.7^8.8^4.9^2\}\{4^5.5\}\{5^3\}_8$.

The frameworks of all of the compounds **1–3** and $\text{ReN}_8\cdot \text{N}_2$ ^[15] are built of a set of standard units: N–N dumbbells, discrete N^{3-} anions and polydiazenediyl chains. An important factor for the stability of the polydiazenediyl chains is a resonance, which imparts partial double-bond character for nitrogen–nitrogen bonds. The stabilization through the resonance is well-known, with the classic examples of azides and pentazolates.^[19] Recently synthesized MgN_4 featuring polydiazenediyl chains could be even recovered at ambient conditions.^[16] Polydiazenediyl chains are also theoretically predicted to exist in CaN_4 , ReN_4 , and $\text{HfN}_8\cdot \text{N}_2$.^[20–23] Along with a pentazolate anion, the polydiazenediyl chain may be one of the most stable structural units to be preserved at ambient pressures.

The compounds **1–3** can be rationalized based on the Mooser–Pearson extended (8–N) rule.^[24] For the polynitride compound MN_x , the number of nitrogen–nitrogen bonds per one nitrogen atom, $b(\text{NN})$, can be calculated as $b(\text{NN}) = (8 - [e(\text{M}) + xe(\text{N})])/x$, where $e(\text{M})$ and $e(\text{N})$ are the numbers of valence electrons of metal and nitrogen, respectively. The results of the calculations applied to polynitrides are presented in the Table 1. It should be noted that $b(\text{NN})$ is fully consistent with the assignments of the bond orders from the crystal-chemical analysis and with the calculated charge density maps (discussed below).

To gain a deeper insight into the electronic properties of the compounds, we calculated the electronic density of states (DOS) and the electron localization function (ELF). At high pressure, all the considered materials are metallic and the

Table 1: Application of the Mooser–Pearson extended (8–N) rule for the description of polynitrides.

Unit	Bonds/atom	Number of atoms belonging to the unit		
		$\text{Hf}_4\text{N}_{20}\cdot \text{N}_2$	$\text{WN}_8\cdot \text{N}_2$	$\text{Os}_5\text{N}_{28}\cdot 3\text{N}_2$
$\text{N}\equiv\text{N}$	3	2	2	6
$[\text{N}_4]_{\infty}^{2-}$	2.5	16	8	16
Polydiazenediyl				
$[\text{N}=\text{N}]^{2-}$	2	2	0	12
$[\text{N}-\text{N}]^{4-}$	1	0	0	0
N^{3-}	0	2	0	0
Av. no. of covalent N–N bonds per N atom (crystal-chemical analysis)		2.27	2.6	2.41
Av. no. of covalent N–N bonds per N atom (the (8–N) rule)		2.27	2.6	2.41

main contribution to the DOS at the Fermi level comes from nitrogen chains (Figure 2) forming delocalized π -bonds, as demonstrated by the spatial distribution of electronic density in the range $-0.1:0$ eV (the inset in Figure 2b shows an example of $\text{WN}_8\cdot \text{N}_2$).

The ELF demonstrates strong covalent bonding between nitrogen atoms: the attractor associated with the N–N bond is located halfway between the atomic spheres (Figure 3 a,c,e). The attractor thickness along the N–N bonds decreases from the nitrogen chains to dumbbells, and to nitrogen molecules. This demonstrates the increase of the bond order (from about 1.25 to 2, and to 3, respectively) that is in a good agreement with the crystal-chemical analysis.

Metal–nitrogen bonds reveal a different type of the ELF maxima. Separated attractors shifted toward the nitrogen atoms are found on the Me–N bond lines suggesting formation of two-center polar covalent bonds. Both discrete nitrogen atoms and those of the dumbbell form three-center Me–N–Me bonds with Os and Hf atoms with slight delocalization. According to the calculated charge density maps (Figure 3 b,d,f), the electron density is nearly similar between all of the atoms of the nitrogen chains with only a slight increase on the bonds parallel to the line connecting the metal atoms compared to the side bonds. This leads to a small difference in the lengths of N–N bonds in polydiazenediyl chains.

Although the synthesis of some porous materials may require high pressure (for example, ZIF-8,^[25] hydrothermal synthesis of zeolites^[26]), the formation of porous structures at megabar pressures seems to be counterintuitive, as these conditions are expected to destabilize less dense framework structures. However, the pressures of about 110 GPa and temperatures of 2000 K are the conditions of the thermodynamic equilibrium between molecular and polymeric nitrogen, thus the volume gain of polymeric nitrogen is balanced by the energy of the triple nitrogen–nitrogen bond.^[27] Furthermore, the polar covalent character of M–N bonds means that polydiazenediyl chains act as classical ligands (as donors for N–Me bonding). This imposes additional restrictions on the geometry of the system, namely, because of the sp^2 hybridization of nitrogen atoms, a metal must be in the same plane as the coordinating nitrogen chain. It is indeed the case for the compounds **1–3** studied in the current work and

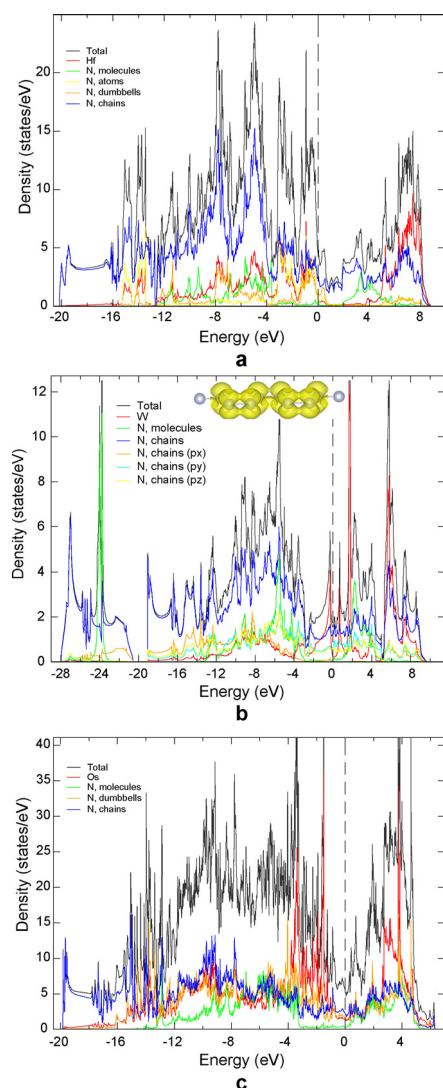


Figure 2. Calculated electronic densities of states for a) $\text{Hf}_4\text{N}_{20}\text{N}_2$ at $P=96.4$ GPa, b) WN_8N_2 at $P=103$ GPa, and c) $\text{Os}_5\text{N}_{28.3}\text{N}_2$ at $P=108$ GPa. The inset in (b) shows a spatial distribution of the electronic density in the range $-0.1:0$ eV on the N atoms of the chains.

ReN_8N_2 ,^[15] which enables us to suggest that the covalent character of the transition metal–nitrogen bonds is one of the important factors for the framework architecture: the imposed geometry constraints lead to the formation of framework structures, rather than to the densest packing of atoms even at ultrahigh pressures. Another factor stabilizing the compounds **1–3** is the inclusion of nitrogen molecules into the pores. Entrapment of a pressure-transmitting medium by metal–organic frameworks upon compression is a well-known phenomenon, which significantly affects their properties, such as compressibility, amorphization pressures, and the sequence of phase transitions.^[28–30]

The synthesis of nitrogen-rich MIFs requires a substantial excess of nitrogen over metal. Owing to the design of the DAC experiment, in which the reagents are initially in different states of aggregation (metal is solid, and nitrogen is gaseous), it is not possible to make a homogenous mixture

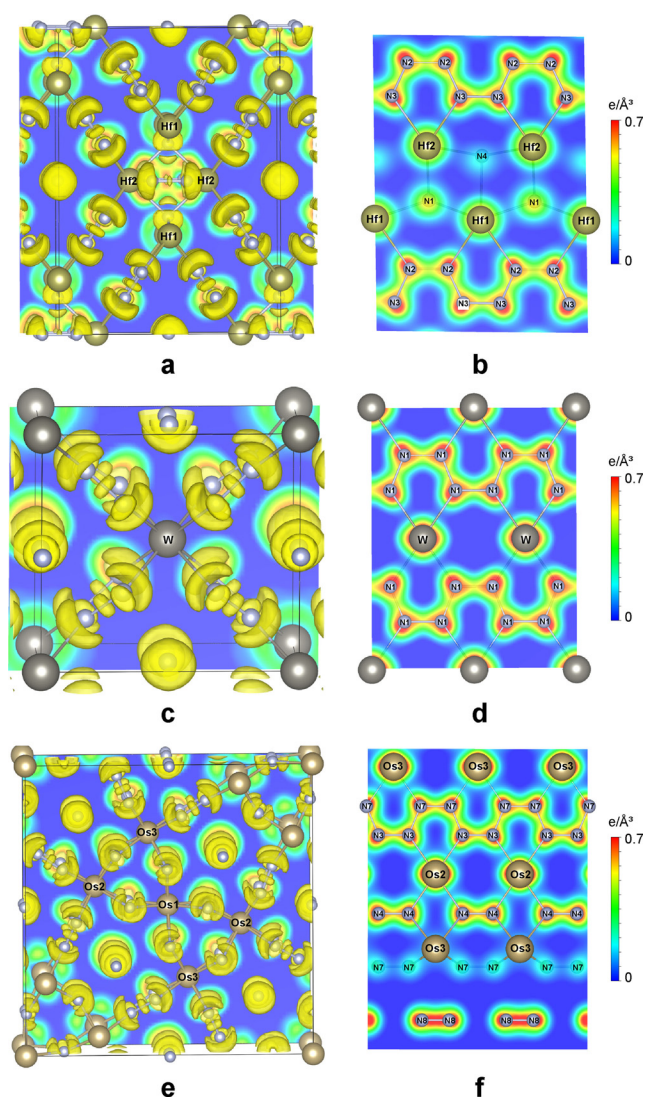


Figure 3. Calculated electron localization function with isosurface value 0.8 (a,c,e) and charge density maps (b,d,f) for $\text{Hf}_4\text{N}_{20}\text{N}_2$ (a,b) at $P=96.4$ GPa, WN_8N_2 (c,d) at $P=103$ GPa, and $\text{Os}_5\text{N}_{28.3}\text{N}_2$ (e,f) at $P=108$ GPa.

with a definite M:N ratio. Therefore, the formation of MIFs happens at the interface between a metal piece and nitrogen (Figure 4), whereas the bulk of the metal sample either remains intact or partially transforms to other nitrides. For example, a considerable part of the Os sample (Figure 4c) turned into osmium pernitride OsN_2 with the marcasite structure type.^[31]

In the Hf–N system, the reaction product, along with $\text{Hf}_4\text{N}_{20}\text{N}_2$, contains a novel compound with a chemical formula Hf_2N_{11} (**4**) (Figure 5; Supporting Information, Tables S3, S4). The structure of Hf_2N_{11} is built of Hf atoms coordinated by discrete nitrogen atoms, N=N dumbbells and catena-poly[*trans*-tetraz-1-ene-1,4-diyl] chains $[-\text{N}=\text{N}-\text{N}-\text{N}-]$ (Figure 5c) similar to those previously observed in FeN_4 .^[13] Discrete nitrogen atoms and dumbbells are within Hf_4 tetrahedra (Figure 5d), while polymeric nitrogen chains form double-helix structure (Figure 5e). Inorganic double

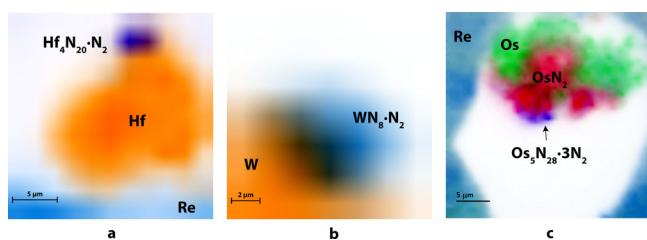


Figure 4. X-ray diffraction imaging maps of samples containing a) $\text{Hf}_4\text{N}_{20}\cdot\text{N}_2$, b) $\text{WN}_8\cdot\text{N}_2$, and c) $\text{Os}_5\text{N}_{28}\cdot 3\text{N}_2$.

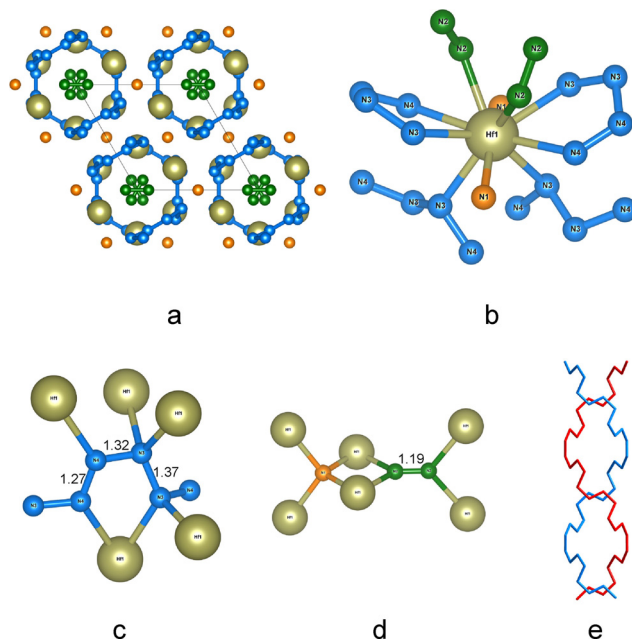


Figure 5. The crystal structure of Hf_2N_{11} . a) View of the crystal structure along the c -axis. Blue: N atoms of the infinite chains, green: N atoms that form dumbbells, orange: discrete N atoms. b) Coordination environment of the Hf atom. c) Coordination environment of polymeric nitrogen chains. d) Coordination environment of discrete nitrogen atoms and nitrogen dumbbells. e) Double-helix chain built of nitrogen atoms running along the c -direction.

helix structures are extremely rare and may have extraordinary properties.^[32,33] The crystal chemical formula of Hf_2N_{11} may be written as $\text{Hf}_2\text{N}(\text{N}_4)_2(\text{N}_2)$. It should be noted that the charge balance is not achieved if the N_2 dumbbell unit has a charge of -2 or -4 . The N–N distance within this unit is 1.186 Å, which is significantly shorter than in $[\text{N}=\text{N}]^{2-}$ or $[\text{N}-\text{N}]^{4-}$. We, therefore, can suggest that Hf_2N_{11} contains N_2^- units with an effective N–N bond order of 2.5. This agrees with the charge balance $(\text{Hf}^{4+})_2\text{N}^{3-}(\text{N}_4^{2-})_2(\text{N}_2^-)$ and with the 8– N rule. Such N_2^- units were recently reported in CuN_2 at high pressure.^[34]

The framework $\text{HfN}_8\cdot\text{N}_2$, isostructural to $\text{WN}_8\cdot\text{N}_2$ and $\text{ReN}_8\cdot\text{N}_2$, was previously predicted by Zhang et al.^[22] The absence of this topology among the Hf compounds we observed in our experiments may have the following explanation. First, whereas WN_8 obeys the 18e rule and ReN_8 , as a 19e complex, shows just a small deviation, the HfN_8 framework would have been a less stable 16e complex (the

same reasoning could also explain why Os does not form a 20e OsN_8 complex). Second, Hf metal has much lower electronegativity and readily forms bonds of more ionic character that explains N^{3-} and N_2^{2-} ions in the crystal structure of $\text{Hf}_4\text{N}_{20}\cdot\text{N}_2$ and Hf_2N_{11} .

Phonon dispersion relations calculated for compounds 2–4 show their dynamic stability at high pressure, as evidenced by the absence of any imaginary phonon modes (Supporting Information, Figures S1–S3). At the same time, the phonon dispersion curves of $\text{WN}_8\cdot\text{N}_2$ (compound 2) and Hf_2N_{11} (4) do have imaginary modes at atmospheric pressure that suggests their instability at ambient pressure and $T=0$ K. Indeed, $\text{WN}_8\cdot\text{N}_2$ produced good diffraction patterns down to about 25 GPa. Further pressure release resulted in an unknown compound with the following lattice parameters: $a = 5.431(5)$, $b = 6.36(7)$, $c = 7.236(9)$ Å, $\alpha = \gamma = 90^\circ$, $\beta = 95.3(1)^\circ$. Unfortunately, the quality of its diffraction pattern did not allow a reliable structure solution. We would like to note that small magnitude of the imaginary frequencies seen in Hf_2N_{11} and $\text{WN}_8\cdot\text{N}_2$ at ambient pressure is expected to be removed at finite temperature by anharmonic effects (renormalization).^[35] Similar argument supports the stabilization of $\text{Hf}_4\text{N}_{10}\cdot\text{N}_2$ at finite temperature even though phonon calculations in the harmonic approximation at $T=0$ K resulted in small imaginary frequencies for some optical modes (Supporting Information, Figure S4).

The decompressed Os–N sample contained only Os and OsN_2 (Supporting Information, Figure S5). The crystal quality of both Hf_2N_{11} and $\text{Hf}_4\text{N}_{20}\cdot\text{N}_2$ deteriorated rapidly on decompression and the diffraction from these compounds was almost undetectable below 80 GPa. In the search of the predicted $\text{HfN}_8\cdot\text{N}_2$ compound at lower pressures, we reheated the sample at 73 GPa.^[22] The resulting material was cubic Hf_3N_4 ($I\bar{4}3d$, No. 220, $a = 6.2946(13)$ Å), as evident from the SCXRD analysis (Supporting Information, Table S5).^[36]

In conclusion, at extremely high pressures we have discovered three novel inclusion compounds, $\text{Hf}_4\text{N}_{20}\cdot\text{N}_2$, $\text{WN}_8\cdot\text{N}_2$, and $\text{Os}_5\text{N}_{28}\cdot 3\text{N}_2$, which are built from host metal–inorganic frameworks and guest dinitrogen molecules. The one-step synthesis of these materials is achieved via a reaction between elemental metal and nitrogen. Their common characteristic structural units, the resonance-stabilized polydiazenediyl (polyacetylene-like) chains, may appear to be appropriate building blocks of other nitrogen-rich compounds that offer an elegant approach to the purposed synthesis of various metal–inorganic frameworks and enables further exploration of the remarkable chemistry of polynitrides.

Acknowledgements

Parts of this research were carried out at the Extreme Conditions Beamline (P02.2) at DESY, a member of Helmholtz Association (HGF). Portions of this work were performed at GeoSoilEnviroCARS (The University of Chicago, Sector 13), Advanced Photon Source (APS), Argonne National Laboratory. GeoSoilEnviroCARS is supported by the National Science Foundation–Earth Sciences (EAR–1634415) and Department of Energy–GeoSciences (DE–

FG02-94ER14466). Several high-pressure diffraction experiments were performed on beamlines ID15B and ID11 at the European Synchrotron Radiation Facility (ESRF), Grenoble, France. Research was sponsored by the Army Research Office and was accomplished under the Cooperative Agreement Number W911NF-19-2-0172. N.D. and L.D. thank the Deutsche Forschungsgemeinschaft (DFG projects DU 954-11/1 and, DU 393-9/2, and DU 393-13/1) and the Federal Ministry of Education and Research, Germany (BMBF, grant no. No. 05K19WC1) for financial support. Theoretical analysis of chemical bonding was supported by the Russian Science Foundation (Project No. 18-12-00492). Support from the Swedish Government Strategic Research Area in Materials Science on Functional Materials at Linköping University (Faculty Grant SFO-Mat-LiU No. 2009 00971), Knut and Alice Wallenberg Foundation (Wallenberg Scholar Grant No. KAW-2018.0194), the Swedish Research Council (VR) grant No. 2019-05600 and the VINN Excellence Center Functional Nanoscale Materials (FunMat-2) Grant 2016-05156 is gratefully acknowledged. The simulations were performed on resources provided by the Swedish National Infrastructure for Computing (SNIC) at the PDC Center for High Performance Computing at the KTH Royal Institute of Technology and at the National Supercomputer Centre at Linköping University.

Conflict of interest

The authors declare no conflict of interest.

Keywords: high-pressure synthesis · inclusion compounds · inorganic double helix · metal–inorganic frameworks · polynitrides

- [1] H. G. Von Schnering, W. Hoenle, *Chem. Rev.* **1988**, *88*, 243–273.
- [2] J. Wang, J.-A. Dolyniuk, K. Kovnir, *Acc. Chem. Res.* **2018**, *51*, 31–39.
- [3] B. A. Steele, E. Stavrou, J. C. Crowhurst, J. M. Zaug, V. B. Prakapenka, I. I. Oleynik, *Chem. Mater.* **2017**, *29*, 735–741.
- [4] C. Zhang, C. Sun, B. Hu, C. Yu, M. Lu, *Science* **2017**, *355*, 374–376.
- [5] W. Zhang, K. Wang, J. Li, Z. Lin, S. Song, S. Huang, Y. Liu, F. Nie, Q. Zhang, *Angew. Chem. Int. Ed.* **2018**, *57*, 2592–2595; *Angew. Chem.* **2018**, *130*, 2622–2625.
- [6] C. Sun, C. Zhang, C. Jiang, C. Yang, Y. Du, Y. Zhao, B. Hu, Z. Zheng, K. O. Christe, *Nat. Commun.* **2018**, *9*, 1269.
- [7] Y. Xu, Q. Wang, C. Shen, Q. Lin, P. Wang, M. Lu, *Nature* **2017**, *549*, 78–81.
- [8] Y. Xu, L. Tian, D. Li, P. Wang, M. Lu, *J. Mater. Chem. A* **2019**, *7*, 12468–12479.
- [9] Y. Xu, Q. Lin, P. Wang, M. Lu, *Chem. Asian J.* **2018**, *13*, 1669–1673.
- [10] M. Arhangelskis, A. D. Katsenis, A. J. Morris, T. Frišić, *Chem. Sci.* **2018**, *9*, 3367–3375.
- [11] F. A. Mautner, R. Cortés, L. Lezama, T. Rojo, *Angew. Chem. Int. Ed. Engl.* **1996**, *35*, 78–80; *Angew. Chem.* **1996**, *108*, 96–98.
- [12] M. A. S. Goher, J. Cano, Y. Journaux, M. A. M. Abu-Youssef, F. A. Mautner, A. Escuer, R. Vicente, *Chem. Eur. J.* **2000**, *6*, 778–784.
- [13] M. Bykov, E. Bykova, G. Aprilis, K. Glazyrin, E. Koemets, I. Chuvashova, I. Kuppenko, C. McCammon, M. Mezouar, V. Prakapenka, et al., *Nat. Commun.* **2018**, *9*, 2756.
- [14] M. Bykov, S. Khandarkhaeva, T. Fedotenko, P. Sedmak, N. Dubrovinskaia, L. Dubrovinsky, *Acta Crystallogr. Sect. E* **2018**, *74*, 1392–1395.
- [15] M. Bykov, E. Bykova, E. Koemets, T. Fedotenko, G. Aprilis, K. Glazyrin, H.-P. Liermann, A. V. Ponomareva, J. Tidholm, F. Tasnádi, et al., *Angew. Chem. Int. Ed.* **2018**, *57*, 9048–9053; *Angew. Chem.* **2018**, *130*, 9186–9191.
- [16] D. Laniel, B. Winkler, E. Koemets, T. Fedotenko, M. Bykov, E. Bykova, L. Dubrovinsky, N. Dubrovinskaia, *Nat. Commun.* **2019**, *10*, 4515.
- [17] I. Kantor, V. Prakapenka, A. Kantor, P. Dera, A. Kurnosov, S. Sinogeikin, N. Dubrovinskaia, L. Dubrovinsky, *Rev. Sci. Instrum.* **2012**, *83*, 125102.
- [18] V. A. Blatov, A. P. Shevchenko, D. M. Proserpio, *Cryst. Growth Des.* **2014**, *14*, 3576–3586.
- [19] K. O. Christe, *Propellants Explos. Pyrotech.* **2007**, *32*, 194–204.
- [20] S. Yu, B. Huang, Q. Zeng, A. R. Oganov, L. Zhang, G. Frapper, *J. Phys. Chem. C* **2017**, *121*, 11037–11046.
- [21] S. Zhu, F. Peng, H. Liu, A. Majumdar, T. Gao, Y. Yao, *Inorg. Chem.* **2016**, *55*, 7550–7555.
- [22] J. Zhang, A. R. Oganov, X. Li, H. Niu, *Phys. Rev. B* **2017**, *95*, 020103.
- [23] Z. Zhao, K. Bao, D. Li, D. Duan, F. Tian, X. Jin, C. Chen, X. Huang, B. Liu, T. Cui, *Sci. Rep.* **2014**, *4*, 4797.
- [24] U. Müller, *Inorganic Structural Chemistry*, Wiley, Chichester, **2006**.
- [25] L. Paseta, G. Potier, S. Sorribas, J. Coronas, *ACS Sustainable Chem. Eng.* **2016**, *4*, 3780–3785.
- [26] C. S. Cundy, P. A. Cox, *Microporous Mesoporous Mater.* **2005**, *82*, 1–78.
- [27] H. Alkhalidi, P. Kroll, *J. Phys. Chem. C* **2019**, *123*, 7054–7060.
- [28] I. E. Collings, E. Bykova, M. Bykov, S. Petitgirard, M. Hanfland, D. Paliwoda, L. Dubrovinsky, N. Dubrovinskaia, *ChemPhysChem* **2016**, *17*, 3369–3372.
- [29] I. E. Collings, A. L. Goodwin, *J. Appl. Phys.* **2019**, *126*, 181101.
- [30] C. L. Hobday, C. H. Woodall, M. J. Lennox, M. Frost, K. Kamenev, T. Düren, C. A. Morrison, S. A. Moggach, *Nat. Commun.* **2018**, *9*, 1429.
- [31] A. F. Young, C. Sanloup, E. Gregoryanz, S. Scandolo, R. J. Hemley, H. Mao, *Phys. Rev. Lett.* **2006**, *96*, 155501.
- [32] D. Pfister, K. Schäfer, C. Ott, B. Gerke, R. Pöttgen, O. Janka, M. Baumgartner, A. Efimova, A. Hohmann, P. Schmidt, et al., *Adv. Mater.* **2016**, *28*, 9783–9791.
- [33] V. Soghomonian, Q. Chen, R. C. Haushalter, J. Zubieta, C. J. O'Connor, *Science* **1993**, *259*, 1596–1599.
- [34] J. Binns, M. E. Donnelly, M. Pena-Alvarez, M. Wang, E. Gregoryanz, A. Hermann, P. Dalladay-Simpson, R. T. Howie, *J. Phys. Chem. Lett.* **2019**, *10*, 1109–1114.
- [35] A. B. Mei, O. Hellman, N. Wireklint, C. M. Schlepütz, D. G. Sangiovanni, B. Alling, A. Rockett, L. Hultman, I. Petrov, J. E. Greene, *Phys. Rev. B* **2015**, *91*, 054101.
- [36] A. Zerr, G. Miehe, R. Riedel, *Nat. Mater.* **2003**, *2*, 185–189.

Manuscript received: February 17, 2020

Revised manuscript received: March 19, 2020

Accepted manuscript online: March 24, 2020

Version of record online: May 8, 2020